pp 1197–1214. © Royal Aeronautical Society 2016
doi: 10.1017/aer.2016.55

Aspect ratio effect on elliptical sonic jet mixing

V. Chauhan
vinayc@iitk.ac.in

S.M. Aravindh Kumar
aravinds@iitk.ac.in

E. Rathakrishnan
erath@iitk.ac.in

Department of Aerospace Engineering
Indian Institute of Technology
Kanpur
India

ABSTRACT

The effects of aspect ratio on elliptical sonic jet decay at different levels of under-expansion has been studied experimentally. Elliptical sonic jets from orifices of same area with aspect ratios (AR) 2, 4 and 6 at nozzle pressure ratios 2 to 5 in steps of 1 have also been studied. A circular jet from an orifice with an area equal to that of elliptical orifice was also studied for comparison. Jet centreline pressure decay, spread and waves present in the jet core were analysed. The results show that the mixing of the elliptical jet is superior to the circular jet, at all the nozzle pressure ratios of the present study. Also, the aspect ratio of the elliptical orifice has a strong influence on the jet mixing. Elliptical jets of aspect ratio 4 and 6 experience a significantly higher mixing than the aspect ratio 2 jet, till the under-expansion level corresponding to Mach disk formation. For higher under-expansion levels, the mixing of AR 4 and 6 jets become inferior to that of the AR 2 jet.

Keywords: elliptical jet; axis-switching; core length; under-expansion; shock cell

Received 26 February 2015; revised 12 November 2015; accepted 4 February 2016; first published online 7 June 2016.

NOMENCLATURE

AR	aspect ratio
D	equivalent diameter
NPR	nozzle pressure ratio, P_0/P_a
P_a	atmospheric pressure
P_e	orifice exit pressure
P_0	settling chamber pressure
P_t	pitot pressure in the jet field
X	coordinate along the jet axis
Y	coordinate along the major-axis
Z	coordinate along the minor-axis

1.0 INTRODUCTION

Under-expanded jets, due to the pressure imbalance, generate a complex shock cell structure in the jet core region. The under-expanded state results in the formation of expansion waves at the jet exit. These waves extend to the free boundary of the jet and reflect as weak compression waves. These compression waves coalesce to form intercepting shocks in the interior of the jet, resulting in the formation of periodic shock cell structures in the core of an under-expanded jet[1]. Several studies have been done on under-expanded jets to understand the complex shock cell structures[2-5]. The shape of these shock structures becomes highly asymmetric for jets issuing from orifice or nozzles of non-circular geometries. As a result, vortices of different sizes form at the jet boundary and the jet spreads differently along different planes[6,7]. Studies on non-circular jets show that the jet encounters fine-scale mixing because the mixing promoting small vortices shed from the corners of the nozzle exit[8,9].

Elliptical jets with smooth and continuously varying radii of curvature fall between circular and non-circular jets such as square and rectangular jets. Due to this continuous variation in the radius of curvature, vortices of continuously varying size would be shed from an elliptical nozzle. These mixed-size vortices promote both large- and small-scale mixing, leading to a faster mixing for an elliptical jet compared to an identical circular jet. Schadow et al[10] studied an elliptical jet with an aspect ratio 3:1 and found enhanced mixing characteristics of the elliptical jet compared to a circular jet at subsonic, sonic and supersonic under-expanded conditions. Quinn[11] showed that the mixing in an elliptical jet issuing from a sharp-edged orifice plate is higher than the mixing from elliptical jets issuing from contoured elliptical nozzles and that of round jets. Using planar particle image velocimetry, Mitchell et al[12] studied a low-aspect-ratio under-expanded elliptical jet and reported that there is vortex bifurcation process at the highest pressure ratio of 4.2, which was previously observed only for jets with higher aspect ratios. Yoon and Lee[13] investigated the near-field structure of an elliptical jet using stereoscopic particle image velocimetry and reported that the entrainment of the elliptical jet was about 1.5% larger than that of an identical round jet.

Besides promoting large- and small-scale mixing, elliptical jets, like other non-circular jets, exhibit the phenomenon of axis-switching. Axis-switching is due to the difference in the spread rates of the jet along different planes normal to the jet axis. As a result of this differential spread rate, the major and minor axes of an elliptical jet switch after a certain distance downstream of the nozzle exit. Many researchers have reported this axis-switching phenomenon in the past. Hussain and Husain[14] observed that the location and number

https://doi.org/10.1017/aer.2016.55 Published online by Cambridge University Press

of axis-switching occurrences were strongly influenced by the initial conditions of the jet. Quinn[15] observed that after two switchings of the major and minor axes, the jet attains an axisymmetric shape at about 30 equivalent slot diameters downstream of the exit plane. Even three axis switches have been observed in elliptical jet[16]. Verma and Rathakrishnan[17] studied the flow and acoustic properties of an under-expanded elliptical slot jet issuing from orifices of a small aspect ratio (AR2) to moderate aspect ratios (AR3 and AR4). Their focus was mainly on the axis-switching and acoustic levels of the jets. The effect of Mach number on the acoustic field of 2:1 elliptic-slot jet was also investigated by Verma and Rathakrishnan[18], but this was only for an aspect ratio of 2:1. Clement et al[19] studied the superiority of Mach 0.6 and 0.8 and correctly expanded sonic elliptical jets issuing from orifices with aspect ratios of 2, 3 and 4. They inferred that the enhanced mixing of the elliptical jet was due to the generation of vortices of varying size along the azimuth of the elliptical section.

From the literature, it is evident that the elliptical jets studied were for low and moderate aspect ratios. These works focused mainly on axis switching to quantify the mixing and acoustic aspects. Also, the orifices studied were confined to aspect ratios only up to 4. Further, the waves present in the jet core have not been addressed in these works. A higher aspect ratio on the order of 6 might play a dominant role in modifying the mixing characteristics of elliptical jets. To have a closer look at this important control parameter, elliptical sonic jets issuing from orifices with aspect ratios of 2, 4 and 6 are studied quantitatively and qualitatively in this investigation. The pressure profiles in the directions normal to the minor and major axes at different locations of the jet axis are analysed. Also, the waves present in the elliptical jet core in the major-axis (*XY*) and minor-axis (*XZ*) planes were visualised to understand the effect of differential mixing in the *XY* and *XZ* planes on the formation Mach disc at NPR 4 and 5 (in the case of a circular sonic jet, Mach disc formation takes place for NPR 4 and above). The effects of the level of expansion at the orifice exit, corresponding to nozzle pressure ratios 2 to 5 in steps of 1, are also considered in the study. Elliptical jet decay of the present study at all nozzle pressure ratios are compared to the decay of an equivalent circular jet.

2.0 EXPERIMENTAL DETAILS

2.1 Jet flow facility

The experiments were conducted in the open jet facility at the High Speed Aerodynamics Laboratory, Indian Institute of Technology, Kanpur, India[20]. The compressed air for the settling chamber was supplied from the storage tank through a control valve. To reduce the flow disturbance caused by the control valve, a mixing length of 2 m was placed between the valve and the settling chamber. The flow was conditioned, by two wire-mesh screens placed within the settling chamber, before entering into the nozzle. The desired NPR was achieved by controlling the settling chamber pressure (P_0), because the backpressure was the atmospheric pressure (P_a) into which the jet was discharging.

2.2 Experimental models

The experimental models used in the present investigation were elliptical orifices of aspect ratio 2, 4 and 6 and a circular orifice; all are of the same exit area. The equivalent diameter (D), defined, as the diameter of a circular orifice of same exit area as the elliptical orifice area, was 10 mm for all the aspect ratios of the present study. The Reynolds numbers based on the equivalent diameter (D) were 2.96×10^5 and 7.39×10^5, respectively, for the minimum and

https://doi.org/10.1017/aer.2016.55 Published online by Cambridge University Press

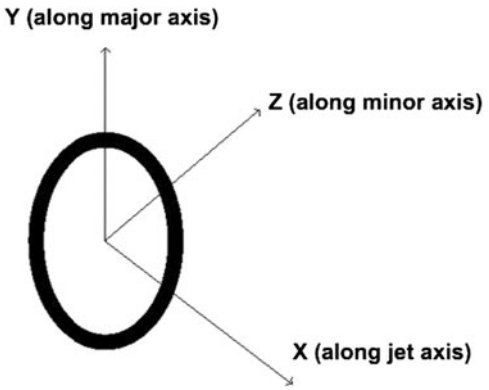

Figure 1. Schematic representation of the coordinate system at the orifice exit.

maximum NPRs of 2 and 5 of the present investigation. A schematic representation of the coordinate system used is shown in Fig. 1.

2.3 Instrumentation

Pitot pressure variation along the jet centreline and along the major axis (Y direction) and minor axis (Z direction) of the orifice, at different axial locations, were measured with a 16-channel Pressure Systems, Inc. 9010 transducer with a range of 0-2.1 MPa. The accuracy of the transducer (after the re-zero calibration) is specified to be ±0.15% full scale.

The pressure measurement in the jet field was done using a pitot tube of 0.4 mm inner diameter and 0.6 mm outer diameter mounted on a rigid three-dimensional traverse with a resolution of 01 mm in linear translation. Thus, the ratio of the orifice exit to the probe area is $(10/0.6)^2 = 277.77$, which is well above the limit of 64 for neglecting the probe blockage effect[20]. In all measurements, the sensing probe stem was kept normal to the jet axis, with its sensing hole facing the flow. Very low Reynolds numbers based on the probe diameter could significantly influence the pressures measured by the pitot probe. However, this effect is seldom a problem in supersonic streams because a probe of reasonable size will usually have a Reynolds number above 500, which is above the range of troublesome Reynolds numbers[22]. Hence, the viscous effect will not cause any error in the pitot pressure measurements. However, it is important to note that the jet pressure field is essentially unsteady due to the vortices prevailing in the flow field. Therefore, what is measured is the mean value of the pitot pressure. In the present study, every measured pitot pressure has an average value of 250 samples per second. The measured values were found to be repeatable within ±3%.

The waves prevailing in the jet core were visualised using a shadowgraph system with a helium spark arc light source in conjunction with a concave mirror. The shadowgraph images were recorded using a still camera.

2.4 Data accuracy

The settling chamber pressure during the experiments of the present investigation was maintained within ±0.5% for all the NPRs studied. The movement of the pitot probe mounted on the traverse had a resolution of ±0.1 mm in the linear translation. The repeatability of the pressure measurements was within ±3%.

https://doi.org/10.1017/aer.2016.55 Published online by Cambridge University Press

3.0 RESULTS AND DISCUSSION

In a supersonic flow, the measured pitot pressure corresponds to the total pressure behind the bow shock in front of the pitot probe and not the actual total pressure[20, 21]. The waves present in the jet core cause the total pressure to vary from point to point. Because of this, it becomes difficult to correct the measured pitot pressure for shock loss. Therefore, for supersonic jets it is not possible to calculate the Mach number or velocity using the measured pitot pressures, as in the case of subsonic jets. Furthermore, in supersonic regions, there is some measurement error due to probe interference with the shock structure. Hence, the results represent only the qualitative nature of the flow in the jet. Nevertheless, the data are accurate enough to capture the overall features of the jet, such as the extent of the supersonic core region, the number of shock cells and the spacing between them[1]. Also, in a steady supersonic flow with a single normal shock wave ahead of the pitot tube, a large pitot pressure corresponds to a low Mach number and vice versa. For supersonic jets, the pitot pressure distribution along the jet centreline can be used to measure the core length of a supersonic jet. The core length can be taken as an indication of the jet mixing: the shorter the core, the better the mixing. The jet decay in the characteristic decay zone and the far field can also be quantified from the centreline pressure decay plots. Thus, without going into the acoustic aspects, the relative mixing of the controlled and uncontrolled jets in the three zones of the jets are analysed with centreline pressure decay results in the present study.

3.1 Centreline pressure decay

The centreline pitot pressure decay is a measure of the mixing of the jet fluid with the fluid entrained. The centreline pressure decay can clearly show the extent of the jet core, which is defined as the axial distance up to which the nozzle exit velocity is unaffected for subsonic jets, and the axial extent up to which supersonic flow prevails for supersonic jets[1].

The pitot pressure (P_t) distribution measured along the jet centreline is non-dimensionalised with the settling chamber pressure (P_0) and plotted against the non-dimensionalised axial distance (X/D). At NPRs 2, 3, 4 and 5, the sonic jet is under-expanded, with under-expansion levels (defined as the ratio of the pressure at the orifice exit (P_e) to the backpressure (P_a)) of 1.05, 1.58, 2.11 and 2.64, respectively. For these levels of under-expansion, expansion waves are formed at the orifice exit to decrease the jet pressure to come to equilibrium with the backpressure, which is the pressure of the atmosphere to which the jet is discharged. Thus, the sonic jet issuing from the orifice is accelerated to higher Mach number by the expansion fan formed at the exit.

The centreline pitot pressure decays of the elliptical jets with aspect ratios of 2, 4 and 6 along with circular jet for NPRs 2 to 5 are compared in Figs. 2-5.

At NPR 2 (Fig. 2), which is almost the correctly expanded state for the sonic jet, there are no oscillations in pitot pressure in the core region. This implies that the waves prevailing in the core are very weak. From Fig. 2, it is seen that the jet core length decreases with an increase in aspect ratio. Among the sonic jets of different ARs studied in the present work, the AR 6 jet has the shortest core followed by a rapid decay in pitot pressure up to $X/D = 8.3$; thereafter, the decay of the AR 2 jet is seen to be better than that for AR 6. The core length in AR 2 and the circular jet are almost the same, but the rate of pressure decay of the AR 2 jet is greater than for the circular jet in the characteristic decay and far field regions. The mixing of the AR 4 jet is faster than that of AR 2 jet in the core region as indicated by a shorter core, but in the characteristic region, the mixing of the AR 4 jet is inferior to that of the AR 2 and AR 6 jets. The core lengths of circular and AR 2 jet are about $X/D = 4.4$, whereas the core length of AR

https://doi.org/10.1017/aer.2016.55 Published online by Cambridge University Press

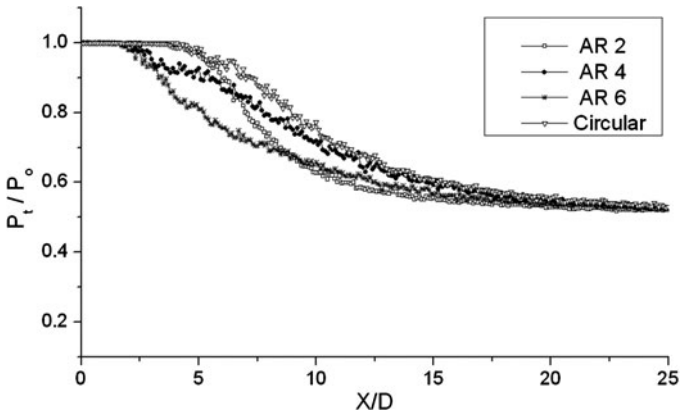

Figure 2. Centreline pitot pressure decay at NPR 2.

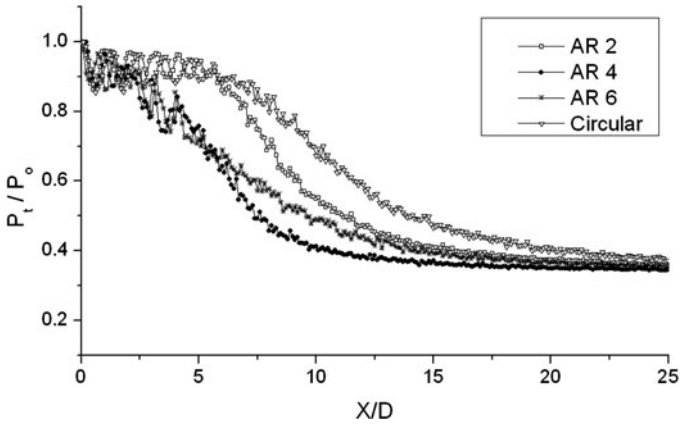

Figure 3. Centreline pitot pressure decay at NPR 3.

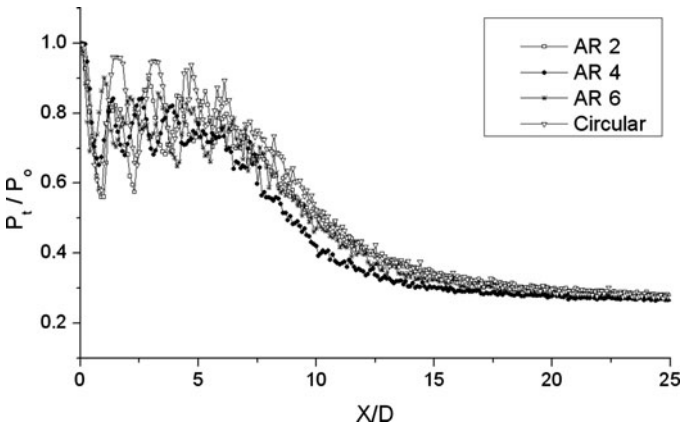

Figure 4. Centreline pitot pressure decay at NPR 4.

https://doi.org/10.1017/aer.2016.55 Published online by Cambridge University Press

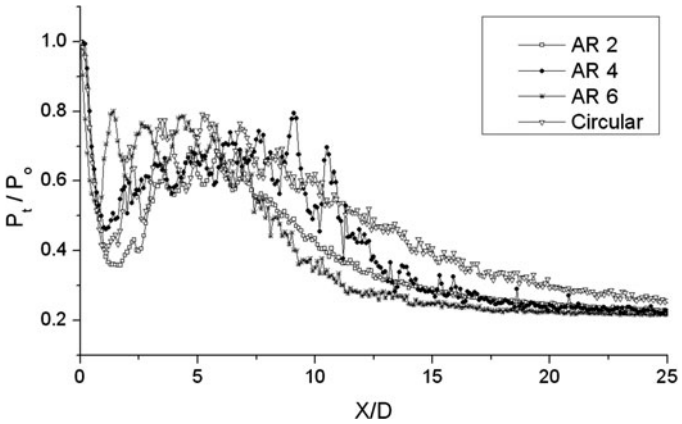

Figure 5. Centreline pitot pressure decay at NPR 5.

6 jet is about $X/D = 2$. Thus the core length reduction caused by AR 6 is about 54% relative to the circular jet. The core length reduction caused by AR 4 is about 43%. This implies that the near-field mixing caused by vortices of continuously varying size from the end of major axis to the end of minor axis in one quadrant of the ellipse of AR 6 is better than that caused by the vortices shed from AR 4. Furthermore, the mixing promotion caused by AR 6 is superior to that for AR 4 even in the characteristic decay. Thus, at the almost correctly expanded state with a favourable pressure gradient of about 5%, AR 6 is a better mixing promoter than the lower aspect ratios.

At NPR 3, waves of considerable strength are present in the core of the jets, as indicated by pronounced oscillations of pitot pressure in the core region (Fig. 3). Five prominent shock cells are present in the core of AR 2 and 6 and circular jet flow fields, whereas the AR 4 jet has only four shock cells. Although the AR 4 and 6 jets have almost the same core length of around $X/D = 4$, the characteristic decay of the AR 4 jet is faster, as indicated by the rapid decrease of the centreline pressure. It is clearly seen from the results that the higher AR jets (AR 4 and 6) have shorter cores and faster decays than the AR 2 jet and the circular jet. Between the AR 2 and circular jets, the decay of AR 2 jet is faster in all the three zones: the core, characteristic decay and the fully developed zone. The shorter core and weaker waves in the core of the AR 4 and 6 jets indicate that the near-field mixing of these jets is faster than for the AR 2 jet. Beyond the core, the AR 4 jet exhibits higher mixing than the AR 6. The AR 4 jet becomes fully developed at about $X/D = 10$, whereas the AR 6 and 2 jets become fully developed only at $X/D = 15$. Thus the aspect ratio of the ellipse has a significant role to play in the mixing of the jet at all three zones. Both AR 6 and 4 result in a core length reduction of about 38% at NPR 3.

The smaller amplitudes of pitot pressure oscillation in the AR 4 and 6 jets at NPR 4 (Fig. 4) relative to larger amplitudes in AR 2 and circular jets are a result of comparatively weaker shock cell structures in the AR 4 and 6 jets. At NPR 4 as seen in Fig. 4, the number of shock cells and the spacing between the shock cells for all the jets is greater than that at NPR 3. Also, the number of shock cells in the elliptical jets is more than that in the circular jet. In contrast to NPR 2 and 3, the core of the AR 6 jet is longer than other jets at NPR 4. Even though the core lengths of the AR 2, AR 4 and circular jets are almost equal, the AR 4 jet experiences better mixing in the characteristic decay zone and far field, as indicated by moderate shock

https://doi.org/10.1017/aer.2016.55 Published online by Cambridge University Press

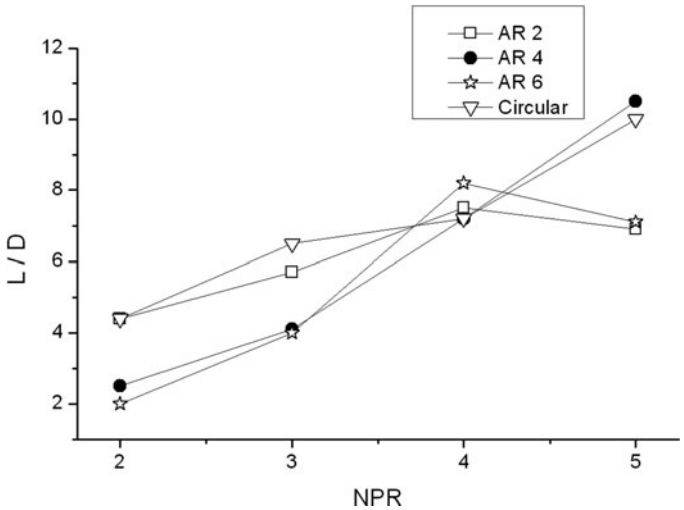

Figure 6. Variation of core length with NPR.

strengths accompanied by rapid decay. At NPR 4, the mixing caused by AR 4 is also superior to that for AR 2 and AR 6 in all the three zones of the jet.

As the NPR increases, a Mach disk begins to form at the end of the first shock cell, as indicated by a larger drop in pitot pressure followed by a rise near the exit of the jet (Fig. 5). Among the jets, the Mach disk for AR 2 is found to be the strongest. After the Mach disk, the downstream shocks in AR 2 jet core becomes weak, while in the circular jet they are still of considerable strength. After the core region, the AR 6 jet decays faster to become fully developed at about $X/D = 14.5$. In the core region of the AR 4 jet, the magnitude of pitot pressure oscillation increases in the downstream direction.

3.2 Core length variation with NPR

The variations in core length with NPR for the jets studied are shown in Fig. 6. The supersonic core length (L) is non-dimensionalised with the equivalent diameter (D). It is seen that for all the elliptical jets and the circular jet, the core length increases with NPR from the almost correctly expanded state (NPR 2) to the NPR at which the Mach disk forms (NPR 4). For an NPR beyond 4 for the AR 4 and circular jets, the core length continues to increase with NPR, whereas for AR 2 and 6, the core length decreases with an increase in NPR. At NPR 2 and 3, the core lengths of AR 4 and 6 jets are much shorter than for AR 2 and circular jets. Beyond NPR 4, the core length of AR 4 becomes significantly larger than the AR 2 and 6, and nearly equal to circular jet core. The core length of AR 6 and AR 2 jet are almost the same at NPR 5. Also, the core length of AR 4 and 6 are the same at NPR 3. At NPR 4, the core lengths of AR 2, 4 and circular jets are almost the same. At NPR 2 the core length of AR 2 jet coincides with the core of circular jet.

From the above results, it is clear that the mixing of elliptical jets is better than that of circular jets at all levels of under-expansion. This is because the size of the vortices generated at the elliptical orifice exit vary continuously from the extremity of the minor axis to the extremity of the major axis in one quadrant, with the largest structure at the minor axis end and the smallest at the major axis end, in accordance with the vortex theory (the size of the vortex

https://doi.org/10.1017/aer.2016.55 Published online by Cambridge University Press

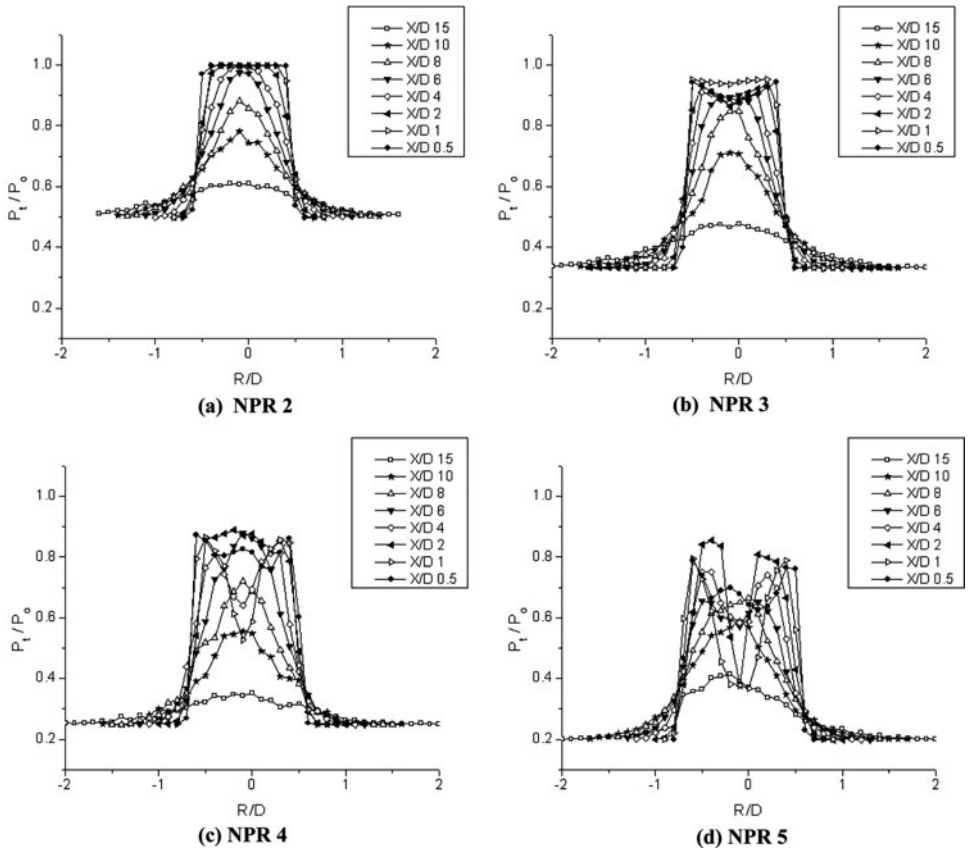

Figure 7. Radial pressure profiles of the circular orifice jet.

leaving a point at the nozzle or orifice exit edge is proportional to the radius of curvature of the edge at that point)[1]. The mixed size of vortices is found to enhance both large-scale and small-scale mixing compared to circular jets where vortices of same sizes form at the orifice exit. The shorter core length and rapid pressure decay in the case of elliptical jets demonstrate the enhanced mixing characteristics of elliptical exit geometries.

3.3 Pressure profiles

To gain an understanding of the jet development and the dependence of axis-switching location on the aspect ratio of the orifice and under-expansion level at the orifice exit, pitot pressure profiles at different axial locations were measured in the *Y-Z* plane.

3.3.1 Circular jet

The pressure variation along the radial direction of circular jet operated at NPRs 2, 3, 4 and 5 at various axial locations is shown in Fig. 7. At NPR 2 (Fig. 7(a)) there is a region of constant pressure around the jet axis, which indicates the radial extent of the potential core region. The weak waves present at NPR 2 in the jet core do not cause any pressure oscillation. After $X/D = 4$, the profiles possess a single peak at the jet centreline and gradually decrease to ambient values as the distance from centreline increases. The axial location at which the jet begins

https://doi.org/10.1017/aer.2016.55 Published online by Cambridge University Press

to exhibit a single peak implies that the mixing initiated at the jet periphery has reached the centreline of the jet and marks the end of core region.

At NPR 3 (Fig. 7(b)), the off-centre peaks in the pressure profiles in the near field are due to the shock cell structure in the jet core. At $X/D = 1$, which is just downstream of the first shock crossover point, the flow attains subsonic value near the centreline (just behind the crossover point) and the pitot pressure is almost constant in that region. The occurrence of single-peak and continuous decrease in pressure at $X/D = 8$ indicates that the supersonic regime is over (with absence of shock structures) and the flow has become subsonic.

As the NPR increases to higher values (NPR 4 and 5), the under-expansion level at the jet exit becomes high and the pressure profiles become more asymmetric as shown in Figs. 7(c) and (d). The magnitude of the dip at the centre of the pressure profiles at some axial locations in the core region increases, which is due to the stronger shock cell strength at these NPRs, as higher expansion is required in a bid to equalise the jet exit pressure and ambient pressure.

3.3.2 Elliptical jets

The pressure profiles of elliptical orifice jets, in minor and major axis planes, at various axial locations are shown in Figs. 8 to 10. From these plots, it is clear that the elliptical jets spread asymmetrically. The jet grows faster along the minor axis compared to the major axis. The shear layer in the major axis plane spreads inward towards the centreline, while at the minor axis plane it spreads both inward and outward. At some axial location from the orifice exit, the width of the jet along the minor axis becomes more than the width along the major axis. This is the location where axis-switching takes place. After this location, the jet continues to grow faster in the minor axis plane up to $X/D = 15$ and the jet does not experience any second axis-switching.

3.3.2.1 AR 2 elliptical jet

The pressure profiles for the AR 2 elliptical jet are shown in Fig. 8. At NPR 2 (Figs. 8(a) and (b)), the jet has constant pressure profiles in the core region. The radial extent of this constant pressure region gradually decreases with increasing axial distance. The single peak pressure profiles after $X/D = 4$ mark the end of the jet core region, and the pressure decays gradually from the centreline to the jet outer edge. The jet width in the major axis plane remains almost constant up to $X/D = 8$ and then it starts increasing slowly. At NPR 2, the jet width along both the axes becomes equal at $X/D = 2$, and the elliptical jet of AR 2 switches axes, between $X/D = 2$ and 4. After this, the jet continues to spread faster along the Z axis without exhibiting any further axis-switching.

The pressure profiles for AR 2 elliptical jet at NPR 3 are shown in Figs. 8(c) and (d). The dips in the pressure profiles in the near field are small, and beyond $X/D = 6$ the pressure gradients become gradual, indicating that the flow has become subsonic. As in the case of NPR 2 and 3, the jet switches axes between $X/D = 2$ and 4.

The pressure profiles for NPR 4 and 5 are shown in Figs. 8(e) to (h). From these results, it is seen that the axis-switching location moves upstream to around $X/D = 2$ with an increase in under-expansion level. This implies that the near-field mixing of the elliptical jet increases with increase of the favourable pressure gradient at the orifice exit. The increase in the level of under-expansion causes the waves in the jet core to become stronger, as indicated by the sharp decrease in the level of pitot pressure in the core.

https://doi.org/10.1017/aer.2016.55 Published online by Cambridge University Press

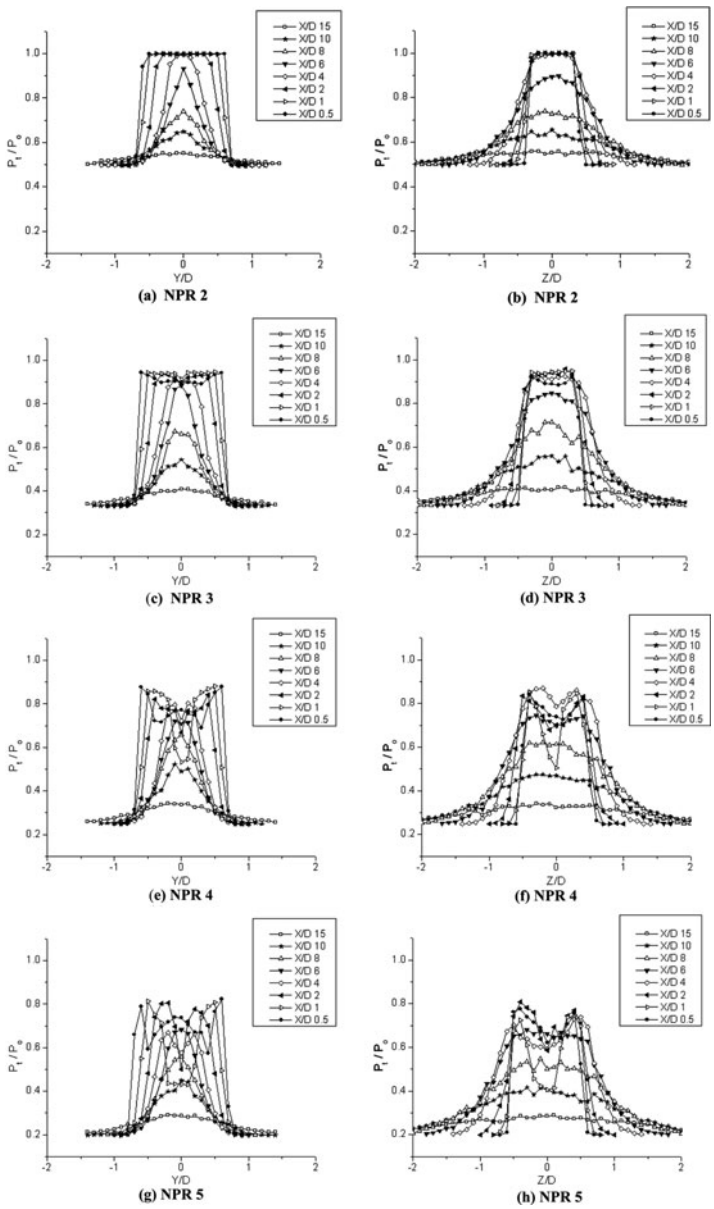

Figure 8. Pressure profiles of the AR 2 elliptical orifice jet along major and minor axes; (a), (c), (e), (g) Y profile; (b), (d), (f), (h) Z profile.

3.3.2.2 AR 4 elliptical jet

The pressure profiles of AR 4 elliptical jet are shown in Fig. 9. The constant pressure width at NPR 2 (Figs. 9(a) and (b)) is more along the major axis, while it is narrower along the minor axis than for the AR 2 jet. This may be because as the aspect ratio increases, the orifice width along the minor axis becomes smaller. This would make the jet boundary along the minor axis

https://doi.org/10.1017/aer.2016.55 Published online by Cambridge University Press

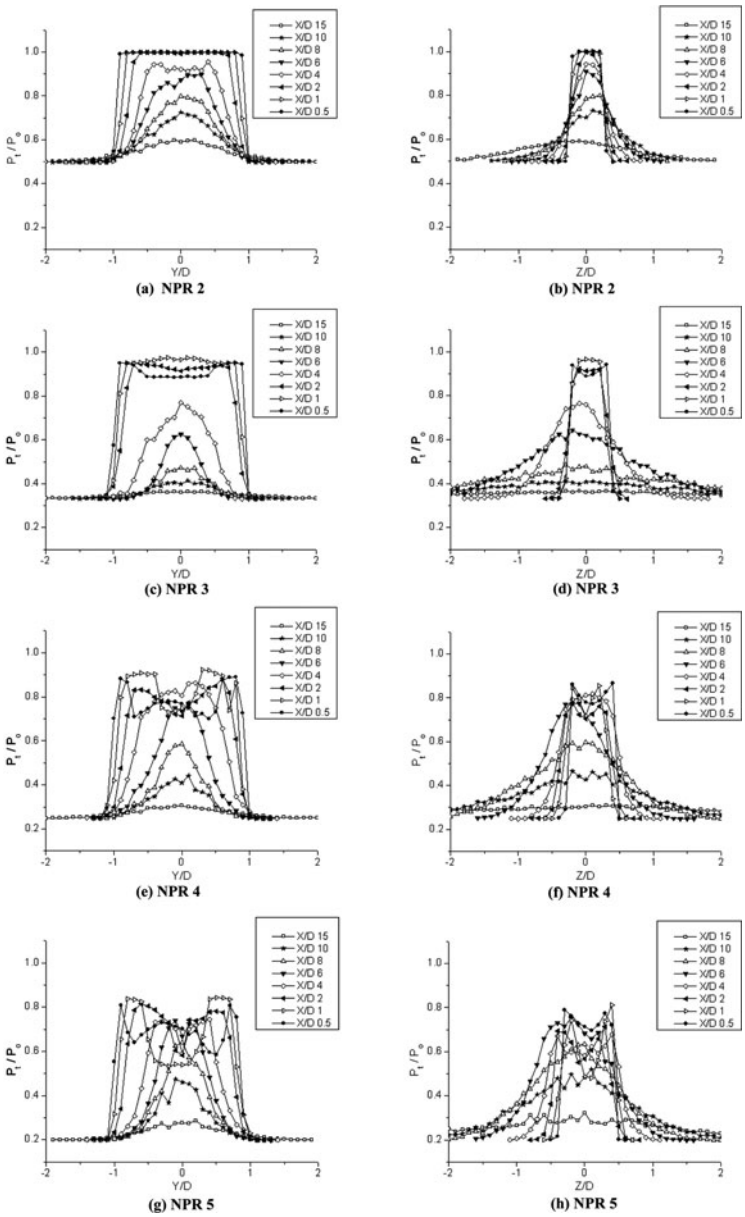

Figure 9. Pressure profiles of the AR 4 elliptical orifice jet along major and minor axes; (a), (c), (e), (g) Y profile; (b), (d), (f), (h) Z profile.

direction get closer to the jet centreline, and this might have enabled the mixing initiated at the jet boundary to reach the jet axis faster compared to lower aspect ratios. The pressure profile at X/D = 15 is similar to circular jet profile and less developed than the AR 2 jet profile. At $X/D = 10$, the jet width along the Y and Z axes becomes equal, and in the far downstream (i.e. at $X/D = 15$), the spread in the Z direction is more than that in Y direction, indicating the occurrence of axis-switching between $X/D = 10$ and 15.

https://doi.org/10.1017/aer.2016.55 Published online by Cambridge University Press

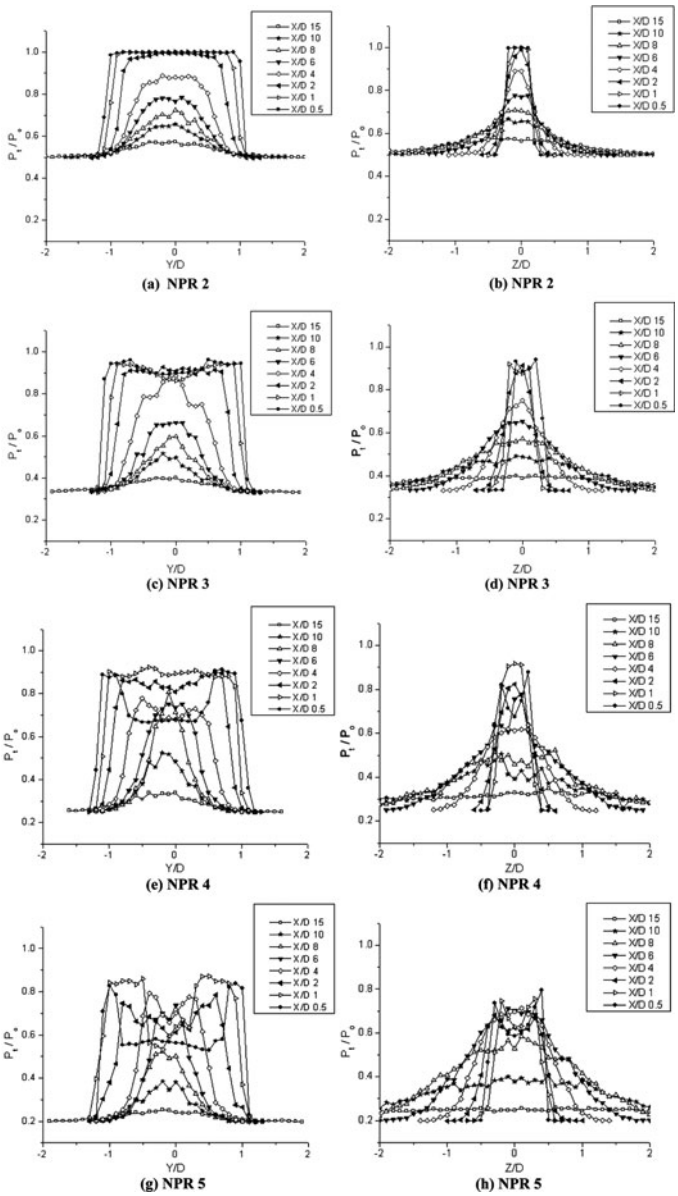

Figure 10. Pressure profiles of AR 6 elliptical orifice jet along the major and minor axes; (a), (c), (e), (g) Y profile; (b), (d), (f),(h) Z profile.

The axis-switching location shifts far upstream to $X/D = 4$ as the NPR increases from 2 to 3. The jet spreads more along the Z direction at NPR 3 compared to NPR 2 and decays completely at about $X/D = 15$, as indicated by the flatter pressure profiles along both the axes.

Increasing the NPR to 4 causes the jet to switch its axes at $X/D = 6$, which is slightly downstream compared to NPR 3. At NPR 5, the jet spread is the same in both the Y and

https://doi.org/10.1017/aer.2016.55 Published online by Cambridge University Press

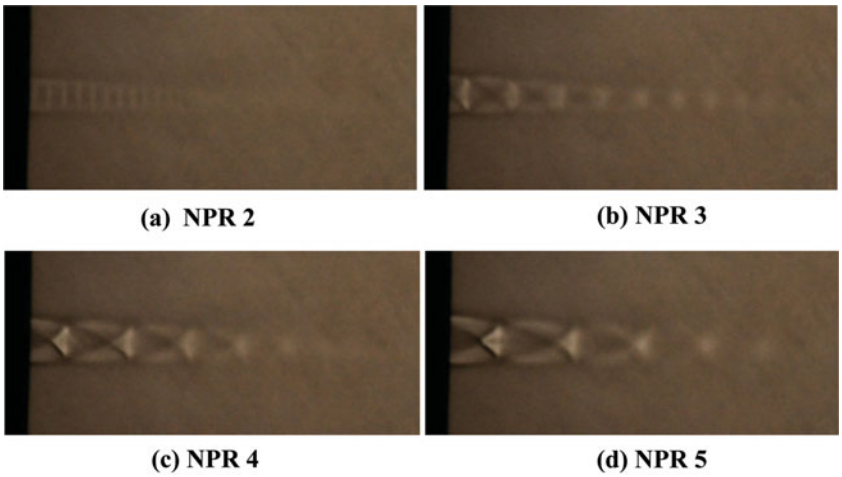

Figure 11. (Colour online) Shadowgraph pictures of the circular jet.

Z directions at $X/D = 4$, and further downstream at $X/D = 6$ the spread in the Z direction becomes more than the Y direction spread. This implies that the axis-switching location does not show any particular trend with NPR in the case of the AR 4 jet.

3.3.2.3 AR 6 elliptical jet

The pressure profiles of the AR 6 jet are shown in Fig. 10. From these figures, it can be seen that the constant pressure width in the core region at NPR 2 is much wider along the major axis compared to the minor axis. At $X/D = 2$, the Z profile shows a single peak, while there is still some constant pressure zone along the Y axis. This implies that the spread of the shear layer towards the jet centreline is faster in the minor-axis plane compared to its spread in the major-axis plane. The jet width at $X/D = 8$ becomes almost equal along both the axes and, as the jet reaches $X/D = 10$, the width along the Z axis becomes more than the width along the Y axis. Therefore, the axis-switching is found to occur between $X/D = 8$ to 10.

The spread in the Z direction increases a little more as the NPR increases to 3. Due to this, the spread along Z direction increases and the axis-switching location shifts to an upstream location of around $X/D = 6$.

The axis-switching location remains at about $X/D = 6$ as NPR increases to 4. With the increase in NPR, the jet spread along the minor axis increases while the increase in NPR does not have any effect on the spreading along the major axis. At NPR 5, the off-centre peaks in the Y profiles are much higher than in the Z profiles. Due to the increased spread along the Z axis at NPR 5, the jet switches axis a little earlier compared to NPR 4. Switching of axes at $X/D = 4$ implies faster mixing and spreading of the jet at NPR 5 than at NPR 4.

The pressure profile results discussed above clearly indicate that the axis-switching location is strongly influenced by the orifice aspect ratio and the under-expansion level at the orifice exit. Increasing the under-expansion level and decreasing the aspect ratio causes the axis-switching location to move upstream.

3.4 Flow visualisation

Figures 11-14 show the shadowgraph pictures of the flow field at NPR 2, 3, 4 and 5. For elliptical jets, images were taken viewing along the major axis (XZ plane) and normal to the

https://doi.org/10.1017/aer.2016.55 Published online by Cambridge University Press

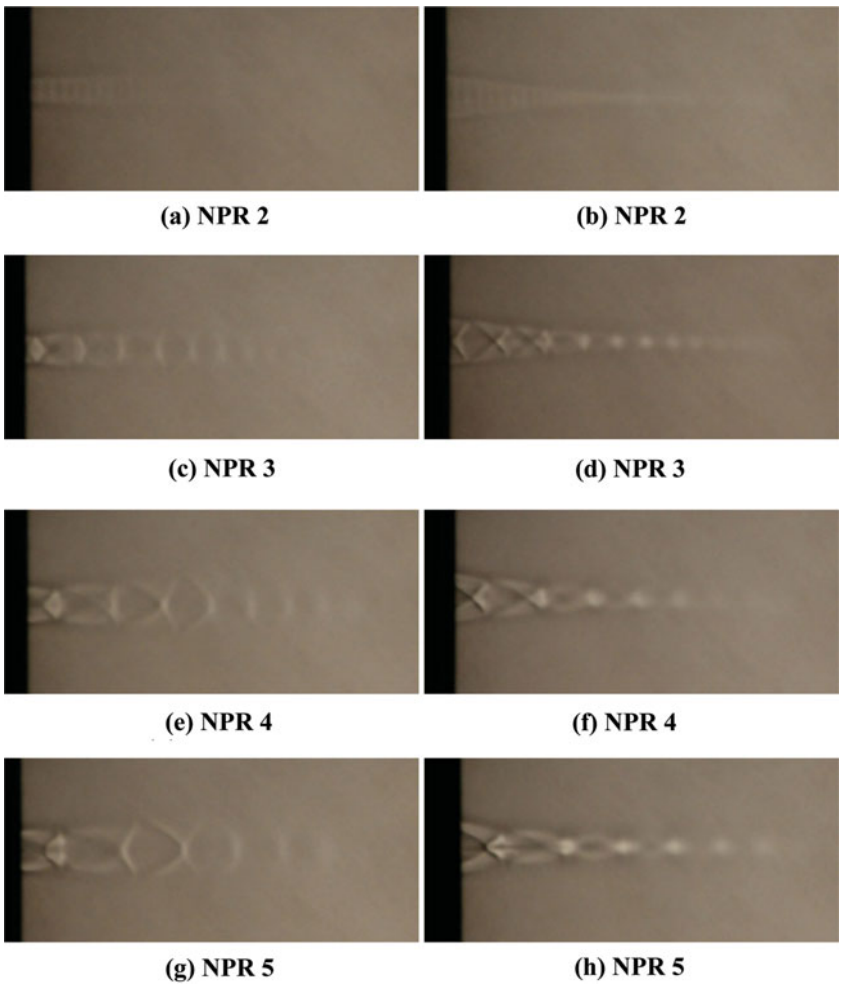

Figure 12. (Colour online) Shadowgraph pictures of the AR 2 orifice jet; (a), (c), (e) and (g) viewed along the major axis (XZ plane); (b), (d), (f), and (h) viewed along the minor axis (XY plane).

major axis (*XY* plane). From these images, it is clearly seen that the shock cell structures converge in the major axis plane and diverge in the minor axis plane of the elliptical jets. This distinct nature of the shock cell structures along these two planes supports the observations based on the pitot pressure profiles. Since all the operating conditions correspond to an under-expanded state at the exit, expansion waves are formed at the edge of the orifice. The expansion waves extend to the boundary of the jet and reflect as compression waves. These compression waves coalesce to form the intercepting shock in the interior of the jet, and thus the core of the under-expanded jet is dominated by periodic shock cell structure.

The low under-expansion level ($P_e/P_a = 1.05$) at NPR 2 results in the formation of weak waves in the jet core. These weak waves cause some light bright and dark regions in the circular and elliptical jet core. Above NPR 2, the periodic shock cell structure begins to appear in the jet core. This shock structure gradually gets diffused in the downstream direction due to the mixing arising from the shear layer spreading towards the jet centreline

https://doi.org/10.1017/aer.2016.55 Published online by Cambridge University Press

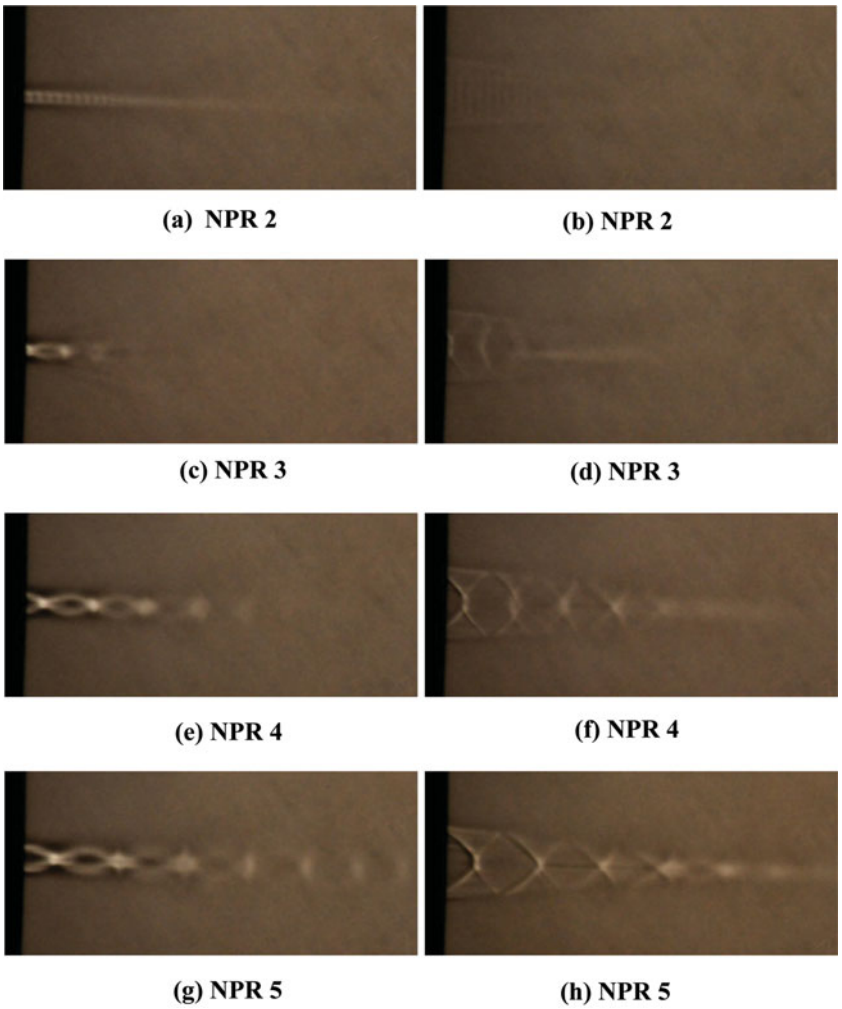

Figure 13. (Colour online) Shadowgraph pictures of the AR 4 orifice jet; (a), (c), (e) and (g) viewed along the majoraxis (XZ plane); (b), (d), (f) and (h) viewed along the minor axis (XY plane).

and the surroundings. The shorter core lengths and weaker shock structure of AR 4 and 6 jets compared to AR 2 and circular jets observed in the centreline pressure decay at NPR 3 can be seen in the shadowgraph pictures. As the NPR increases, the lengths of first three to four shock cells, which are identifiable in these images, also increase. At NPRs 4 and 5, the strong expansion waves at the orifice exit lead to Mach disk formation in the first cell. For the AR 4 and 6 jets, two such Mach disks are observed at NPR 5 in the major axis plane. It is seen that the Mach disk size is distinctly different in the major and minor axis planes.

4.0 CONCLUSIONS

Elliptical jets are found to be effective in enhancing mixing compared to circular jets at all levels of under-expansion studied in this work. The shorter core lengths followed by a rapid

https://doi.org/10.1017/aer.2016.55 Published online by Cambridge University Press

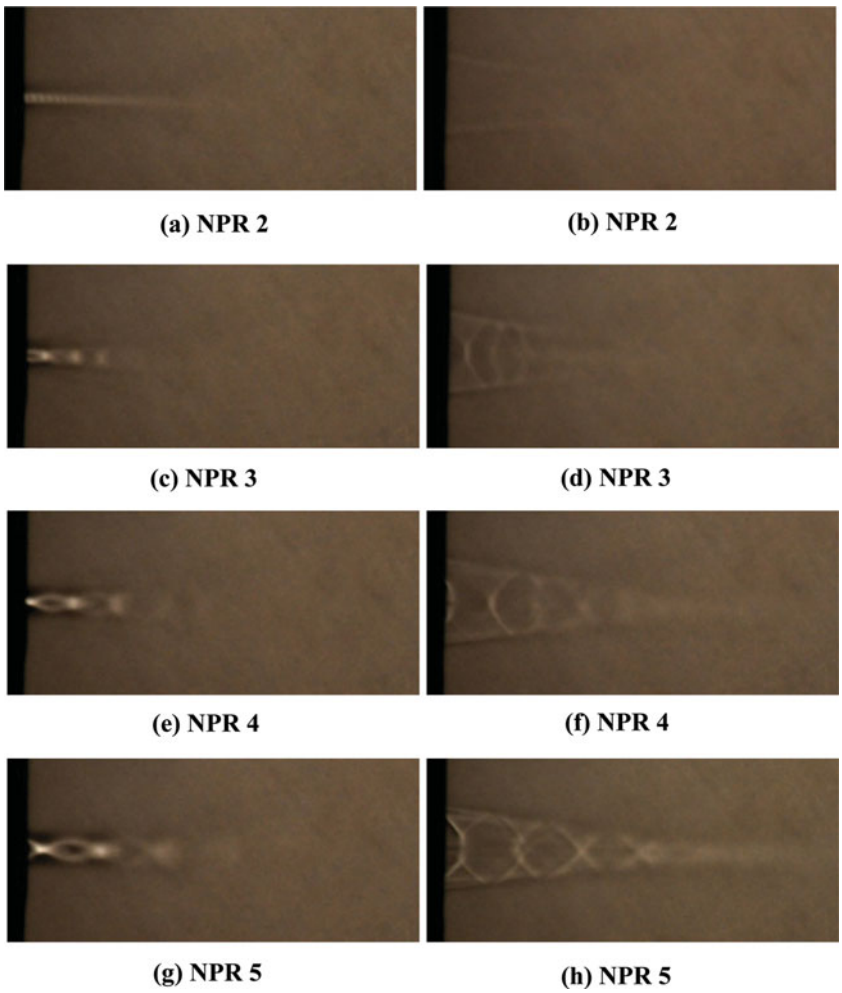

Figure 14. (Colour online) Shadowgraph pictures of the AR 6 orifice jet; (a), (c), (e) and (g) viewed along the major axis (XZ plane); (b), (d), (f) and (h) viewed along the minor axis (XY plane).

decay of pitot pressure demonstrate the mixing superiority of elliptical jets. Pressure profile plots along the major and minor axis sides indicate the asymmetrical and faster spread of elliptical jets. This asymmetrical spread of elliptical jets results in axis-switching, and the distance from the orifice exit where axis-switching takes place depends on the orifice aspect ratio and expansion level of the jet. Increasing the favourable pressure gradient at the orifice exit results in the upward shifting of the axis-switching location, indicating the increase in the near-field mixing. The lesser amplitudes of pitot pressure oscillation in elliptical jet core indicate that the shock cell structure of elliptical jet is weaker than that of circular jet.

REFERENCES

1. RATHAKRISHNAN, E. *Applied Gas Dynamics*, John Wiley, NJ, 2010.

https://doi.org/10.1017/aer.2016.55 Published online by Cambridge University Press

2. HATANAKA, K. and SAITO, T. Influence of nozzle geometry on underexpanded axisymmetric free jet characteristics, *Shock Waves*, 2012, **22**, pp 427-434.
3. DOSANJH, D.S. and SHEERAN, W.J. Observations on jet flows from a two-dimensional underexpanded sonic nozzle, *AIAA J*, 1968, **6**, (3), pp 540-542.
4. GRIST, S., SHERMAN, P.M. and GLASS, D.R. Study of the highly underexpanded sonic jet, *AIAA J*, 1966, **4**, (1), pp 68-71.
5. DAVIDOR, W. and PENNER, S.S. Shock standoff distances and Mach-disk diameters in underexpanded sonic jets, *AIAA J*, 1971, **9**, (8), pp 1651-1653.
6. GRINSTEIN, F.F., GUTMARK, E. and PARR, T. Near field dynamics of subsonic free square jets:a computational and experimental study, *Physics of Fluids*, 1995, **7**, (6), pp 1483-1497.
7. GUTMARK, E., SCHADOW, K.C. and WILSON, K.J. Subsonic and supersonic combustion using noncircular injectors, *J Propulsion*, 1991, **7**, (2), pp 240-249.
8. MILLER, R.S., MADNIA, C.K. and GIVI, P. Numerical simulation of non-circular jets, *Computer & Fluids*, 1995, **24**, (1), pp 1-25.
9. KOSHIGOE, S., GUTMARK, E. and SCHADOW, K.C. Initial development of noncircular jets leading to axis-switching, *AIAA J*, 1989, **27**, (4), pp 411-419.
10. SCHADOW, K.C., GUTMARK, E., KOSHIGOE, S. and WILSON, K.J. Combustion-related shear-flow dynamics in elliptical supersonic jets, *AIAA J*, 1989, **27**, (10), pp 1347-1353.
11. QUINN, W.R. Experimental study of the near field and transition region of a free jet issuing from a sharp-edged elliptical orifice plate, *European Journal of Mechanics B / Fluids*, 2007, **26**, pp 583-614.
12. MITCHELL, D.M., HONNERY, D.R. and SORIA, J. Near-field structure of underexpanded elliptical jets, *Exp Fluids*, 2013, **54**, p 1578.
13. YOON, J.H. and LEE, S.J. Investigation of the near-field structure of an elliptical jet using stereoscopic particle image velocimetry, *Measurement Science & Technology*, 2003, **14**, pp 2034-2046.
14. HUSSAIN, F. and HUSAIN, H.S. Elliptical jets, Part 1, Characteristics of unexcited and excited jets. *Journal of Fluid Mechanics*, 1989, **208**, pp 257-320.
15. QUINN, W.R. On mixing in an elliptical turbulent free jet, *Physics of Fluids*, 1989, **1**, (10), pp 1716-1722.
16. HO, C.M. and GUTMARK, E. Vortex induction and mass entrainment in a small aspect-ratio elliptical jet, *J Fluid Mechanics*, 1987, **179**, pp 383-405.
17. VERMA, S.B. and RATHAKRISHNAN, E. Flow and acoustic properties of underexpanded elliptic-slot jets, *J Propulsion and Power*, 2001, **17**, pp 49-57.
18. VERMA, S.B. and RATHAKRISHNAN, E. Effect of Mach number on the acoustic field of 2:1 elliptic-slot jet, *Aeronautical J*, 2001, **105**, pp 9-16.
19. CLEMENT, S., MURUGAN, K.N. and RATHAKRISHNAN, E. Superiority of elliptical jets, *J Institution of Engineers (India)*, May 2005, **86**, pp 1-7.
20. RATHAKRISHNAN, E. Experimental studies on the limiting tab, *AIAA J*, 2009, **47**, (10), pp 2475-2485.
21. KATANODA, H., MIYAZATO, Y., MASUDA, M. and MATSUO, K. Pitot pressures of correctly-expanded and underexpanded free jets from axisymmetric supersonic nozzles, *Shock Waves*, **10**, (2), 2000, pp 95-101.
22. RATHAKRISHNAN, E. *Instrumentation, Measurements, and Experiments in Fluids*, CRC Press, Boca Raton, Florida, USA, 2007.

https://doi.org/10.1017/aer.2016.55 Published online by Cambridge University Press